Apolipoprotein A-I mimetics attenuate macrophage activation in chronic treated HIV

William Mu[a,b], Madhav Sharma[a], Rachel Heymans[a], Eleni Ritou[a], Valerie Rezek[b], Philip Hamid[a,b], Athanasios Kossyvakis[a], Shubhendu Sen Roy[a], Victor Grijalva[c], Arnab Chattopadhyay[c], Jeremy Papesh[c], David Meriwether[c], Scott G. Kitchen[b], Alan M. Fogelman[c], Srinivasa T. Reddy[c,d,e,f] and Theodoros Kelesidis[a]

Objective(s): Despite antiretroviral therapy (ART), there is an unmet need for therapies to mitigate immune activation in HIV infection. The goal of this study is to determine whether the apoA-I mimetics 6F and 4F attenuate macrophage activation in chronic HIV.

Design: Preclinical assessment of the in-vivo impact of Tg6F and the ex-vivo impact of apoA-I mimetics on biomarkers of immune activation and gut barrier dysfunction in treated HIV.

Methods: We used two humanized murine models of HIV infection to determine the impact of oral Tg6F with ART ($HIV^+ART^+Tg6F^+$) on innate immune activation (plasma human sCD14, sCD163) and gut barrier dysfunction [murine I-FABP, endotoxin (LPS), LPS-binding protein (LBP), murine sCD14]. We also used gut explants from 10 uninfected and 10 HIV-infected men on potent ART and no morbidity, to determine the impact of ex-vivo treatment with 4F for 72 h on secretion of sCD14, sCD163, and I-FABP from gut explants.

Results: When compared with mice treated with ART alone (HIV^+ART^+), $HIV^+ART^+Tg6F^+$ mice attenuated macrophage activation (h-sCD14, h-sCD163), gut barrier dysfunction (m-IFABP, LPS, LBP, and m-sCD14), plasma and gut tissue oxidized lipoproteins. The results were consistent with independent mouse models and ART regimens. Both 4F and 6F attenuated shedding of I-FABP and sCD14 from gut explants from HIV-infected and uninfected participants.

Conclusion: Given that gut barrier dysfunction and macrophage activation are contributors to comorbidities like cardiovascular disease in HIV, apoA-I mimetics should be tested as therapy for morbidity in chronic treated HIV.

AIDS 2021, **35**:543–553

Keywords: apolipoprotein A-I mimetic peptides, chronic treated HIV, immune activation

[a]Division of Infectious Diseases, [b]Division of Hematology and Oncology, [c]Division of Cardiology, Department of Medicine, David Geffen School of Medicine, [d]Department of Molecular and Medical Pharmacology, [e]Molecular Toxicology Interdepartmental Degree Program, University of California Los Angeles, and [f]Department of Obstetrics and Gynecology, David Geffen School of Medicine, University of California Los Angeles, Los Angeles, California, USA.

Correspondence to Theodoros Kelesidis, MD, PhD, Division of Infectious Diseases, Department of Medicine, David Geffen School of Medicine at UCLA, 10833 Le Conte Ave. CHS 37-121 Los Angeles, CA 90095, USA.

E-mail: tkelesidis@mednet.ucla.edu

Received: 11 June 2020; revised: 26 October 2020; accepted: 18 November 2020.

DOI:10.1097/QAD.0000000000002785

Introduction

Despite antiretroviral therapy (ART), chronic treated HIV is a state of inflammation and immune activation driven by impaired gut integrity in which alterations in microbiome, endotoxin (LPS), oxidized lipids, gut monocytes/macrophages (M/M), and enterocytes are associated with immune activation [1]. Innate immunity biomarkers including IL-6, soluble CD14 (sCD14) and sCD163, and biomarkers of gut barrier dysfunction including intestinal fatty acid-binding protein (I-FABP), are predictors of morbidity in chronic treated HIV [1–3]. M/M rather than T-cell activation is considered a more clinically relevant predictor of morbidity in chronic treated HIV [1–3]. Pending results from clinical trials, it is unclear whether statins can be used as prevention for development of comorbidities like atherosclerotic cardiovascular disease (CVD) in HIV [4]. Thus, there is an enormous unmet need for novel therapeutic strategies in chronic treated HIV.

Apolipoprotein A-I (apoA-I) mimetic peptides bind bioactive lipids with higher affinity than apoA-I and have emerged as a new class of therapeutic molecules for treating inflammatory diseases I [5]. One of these peptides named 6F that is expressed as a transgene in tomatoes, when concentrated (Tg6F) and administered orally, attenuates several inflammatory diseases including cancer, cardiovascular, and inflammatory bowel diseases in mice [6–9]. Tg6F is not taken up systemically, works primarily in the gut and inhibit gut inflammation and M/M activation [6–9]. Tg6F is not yet available in the clinic and preclinical studies, and is needed to validate its impact on inflammation in HIV. Another apoA-I mimetic peptide called 4F can also attenuate gut inflammation in murine models of gut inflammation when given orally [9] and has been shown to be well tolerated in humans when given orally [10] or parenterally [11]. We have previously shown that 4F improved ex-vivo antioxidant/anti-inflammatory activities of HDL from HIV-1-infected individuals with suppressed viremia on potent ART [12]. In this report, we tested whether the apoA-I mimetic peptides Tg6F and 4F may attenuate M/M activation in chronic treated HIV.

Macaque models have limitations (i.e. cost) [13]. HIV transgenic rats do not recapitulate actual HIV infection [14]. The humanized mouse termed the bone marrow/liver/thymus (BLT) mouse offers human stem cell reconstitution in all tissues including the gut, can sustain HIV infection and functional human immune responses (e.g. M/M function) can be studied [15,16]. However, although humanized mice have adequate reconstitution of human cells in gut tissue [15,16] and have been used to study gut barrier dysfunction in HIV [17], most mice develop graft-versus-host disease (GVHD) that may impact the gut and complex effects of HIV, ART, and GVHD on immune cells may not be easily dissected. Chronic infection in the setting of oral potent ART can be maintained in the GVHD-resistant C57BL/6 recombination activating gene 2 (*Rag2*)γcCD47 triple knockout (TKO)-BLT mouse over extended periods [18–20]. The TKO BLT mouse model has adequate reconstitution of human cells in tissues including the gut [18–20]. Thus, given the limitations of humanized mouse models [15–20] and that Tg6F is not yet available for clinical trial, we used independent mouse models (NSG and TKO BLT mice) to test the effect of Tg6F in chronic treated HIV. Finally, we validated in human gut explants from HIV-infected participants whether 4F that has been tested in humans [10,11] and can be translated for clinical use in HIV, attenuates ex-vivo shedding of biomarkers, such as sCD163, sCD14, and I-FABP by gut explants.

We demonstrate for the first time that Tg6F reduces biomarkers of macrophage activation (sCD14, sCD163), gut barrier dysfunction (m-IFABP, m-sCD14) and plasma and gut tissue-oxidized lipoproteins in mouse models of treated HIV. 4F and 6F also attenuated shedding of sCD163, sCD14, and I-FABP by gut explants from HIV-infected participants. Our data, for the first time, provide proof of concept that therapeutic targeting of oxidized lipoproteins, microbial products, and gut barrier dysfunction may improve immune activation that drive morbidity in chronic treated HIV.

Methods

Details are described in Supplemental Material, http://links.lww.com/QAD/B945.

Materials

Transgenic tomatoes expressing the 6F peptide or control empty vehicle tomatoes were grown and freeze–dried as described previously [6]. D-4F and 6F peptides were synthesized as previously [9]. All other materials were purchased from commercially available sources.

Mice

TKO or NSG BLT mice were all generated, bred, and maintained as described [19,21]. All animal protocols were carried out in accordance with all federal, state, and local-approved guidelines. A total of five (two TKO and three NSG) independent cohorts of mice (each constructed from the same donor tissues) were used in this study for various experiments and were pooled for comparing mice that were uninfected (group A: HIV^-), infected and on potent ART (group B: HIV^+, antivirals) and infected on potent ART and Tg6F (group C: HIV^+, antivirals, Tg6F).

HIV infection

Between 16 and 18 weeks, mice were challenged intraperitoneally with 500 ng p24 of HIV-1 89.6 virus as described previously [15,16].

Antiretroviral treatment

TKO C57 Bl6 mice were treated with ARVs consisted of combination medication of abacavir/dolutegravir/lamivudine (Triumeq) resuspended in the sweetened water gel formulation (Medidrop Sucralose) as previously described [22]. NSG BLT mice were treated with ART regimen consisting of tenofovir disoproxil fumarate (TDF, 8.75 mg/kg)/emtricitabine (FTC, 13 mg/kg)/raltegravir (RAL, 17.5 mg/kg). See Supplemental material, http://links.lww.com/QAD/B945 for details.

Study participants

HIV-seronegative ($n = 10$) and seropositive ($n = 10$) 50–60 years old participants were recruited in the Gastroenterology Unit of UCLA. To avoid confounding effects from sex [23], race, inflammation (other than HIV) on M/M activation, we selected HIV^+ white men, with no known clinical disease other than HIV or risk factors for clinical disease (e.g. metabolic syndrome, diabetes, dyslipidemia, use of lipid-lowering medication). Six participants were on elvitegravir, cobicistat, emtricitabine (FTC), tenofovir alafenamide (TAF), and four participants were on bictegravir/FTC/TAF. All HIV-infected persons had suppressed viremia (HIV-1 RNA <50 copies/ml), $CD4^+$ T cells greater than 500 cells/μl, duration of ART therapy between 3.2 and 6.5 years and nadir $CD4^+$ T-cell count greater than 250 cells/μl. Ten healthy white men were also included. All individuals enrolled in the study provided written informed consent and the study was approved by the local Institutional Review Board.

Gut explants

Biopsy specimens were obtained endoscopically from the rectosigmoid colon and gut mucosal explants were processed as previously described [24].

Apolipoprotein A-I mimetics

For studies involving Tg6F, the final diets contained 0.06% of Tg6F extract by weight and were administered for 12 weeks as previously described [6,7]. Triplicate biopsies were treated with 4F, 6F, or sham peptide at concentration 100 μg/ml for 72 h as previously described [9].

Biomarkers of barrier permeability and immune activation

Human biomarkers of immune activation were determined in BLT mouse plasma and supernatants from human gut explants using the human magnetic Luminex assay kits according to the manufacturer (R&D, Minneapolis, Minnesota, USA). LBP and I-FABP were quantified using ELISA (R&D). Plasma LPS, sCD14, LBP, IFABP were determined in mice as biomarkers of intestinal barrier function as previously described [17].

Determination of oxidized lipoproteins

Plasma and gut tissue levels of oxidized HDL and LDL were determined by ELISA (MyBioSource, San Diego, California, USA). Oxidized HDL was also determined using a fluorometric biochemical assay that measures HDL lipid peroxidation (HDLox) [25].

Statistics

P values less than 0.05 by Kruskal–Wallis or Mann–Whitney were considered significant. For all correlations, Spearman's correlation coefficient was calculated. All analyses were performed with Graphpad, version 7.0 (Graphpad Software, San Diego, California, USA).

Results

Independent antiretroviral therapy regimens have similar impact on viral load and human immune cells in bone marrow/liver/thymus models of HIV

Cellular immune responses in BLT mice infected with HIV closely mirror those in humans, making it a good model to study HIV immune disorder *in vivo* [14–16]. We generated two independent (TKO and NSG) BLT models (Fig. 1a and b) of humanized mice with identical functional human M/M [16,18] (for representative flow plots of human immune cells, see Supplemental Figure 1, http://links.lww.com/QAD/B945; supplemental material available online with this article) and mock-infected or infected with HIV-1 (HIV^+). We tested two independent contemporary ART regimens and observed that both similarly suppressed plasma viremia and altered h-CD4: h-CD8 T-cell ratio, in both BLT models (Supplemental Figure 2a–d, http://links.lww.com/QAD/B945).

Chronic treated HIV infection increased innate immune activation in bone marrow/liver/thymus models of treated HIV

Using a sensitive Luminex immunoassay platform, we determined whether the BLT mice can be used as model to study *in vivo* the impact of Tg6F on increase in plasma sCD14 and sCD163 in chronic treated HIV [1–3]. Given that variable engraftment of human M/M and cellular activation determine plasma levels of h-sCD14 and h-sCD163 and to better compare results among mice, we determined changes in h-sCD14 and h-sCD163 among mice groups over 16 weeks of potent ART and within the same mice over 30 days on potent ART. HIV^+ART^+ mice infected over 16 weeks had increased h-sCD14 (Fig. 1c) and h-sCD163 (Fig. 1d) compared with HIV^- NSG BLT mice. Within the same mouse cohort, ART did not impact sCD14 and h-sCD163 over 30 days in both NSG (Supplemental Figure 3a and b, http://links.lww.com/QAD/B945) and TKO BLT mice (Supplemental Figure 3c and d, http://links.lww.com/QAD/B945). We also used the BLT mice to study gut barrier dysfunction as instigator of M/M activation in chronic treated HIV [1–3]. Plasma biomarkers of gut barrier

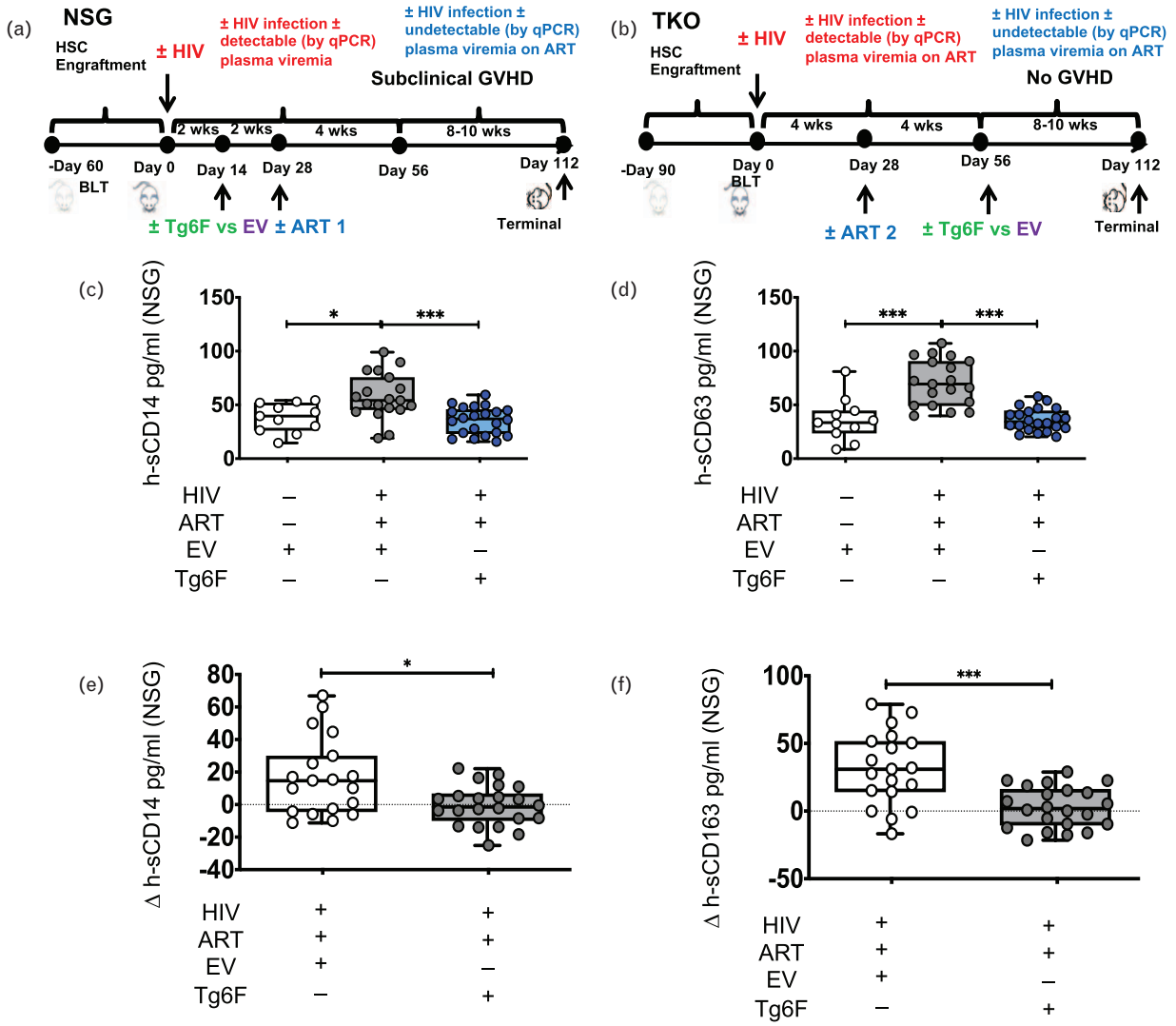

Fig. 1. Tg6F attenuates increase in biomarkers of innate immune activation in humanized mouse models of chronic treated HIV infection. TKO C57 and NSG humanized [bone marrow/liver/thymus (BLT)] mice were constructed, infected and treated with EV, ART, Tg6F, as in methods. Biomarkers of innate immune activation in chronic treated HIV (s-CD14, s-CD163) were determined in plasma by Luminex immunoassays. (a) Study design for NSG mice. Three cohorts of GVHD-prone NSG mice ($n = 52$) without signs of clinical GVHD were pooled. The first group was uninfected without ART, white boxes and datapoints, HIV$^-$ ($n = 11$). The second group was infected and received ART, dark grey boxes and datapoints, HIV$^+$ART$^+$ ($n = 19$). The third group was infected, and received both ART and Tg6F, blue boxes and datapoints, HIV$^+$ART$^+$Tg6F$^+$ ($n = 22$). The uninfected (HIV$^-$) and HIV$^+$ART$^+$ mice were all fed with chow diet that contained control transgenic tomato concentrate (EV) to ensure that the effectiveness of Tg6F is because of the presence of 6F, which is not present in EV. (b) Study design for TKO mice. Two cohorts of GVHD-resistant TKO BLT mice ($n = 38$) were pooled. The order, colors, and symbols are the same as for the NSG BLT mice. The first group was uninfected without ART, HIV$^-$ ($n = 8$). The second group was infected and received ART, HIV$^+$ART$^+$ ($n = 15$). The third group was infected, and received both ART and Tg6F, HIV$^+$ART$^+$Tg6F$^+$ ($n = 15$). To dissect differential effects of Tg6F on biomarkers in treated HIV, Tg6F was given 8 weeks after infection and 4 weeks after ART with confirmation of suppressed viremia (by PCR). Data represent box and whiskers with minimum, median, and maximum values of human sCD14 (h-sCD14) (c) and h-sCD163 (d) in NSG BLT mice ($n = 8$–22 mice per group). (e and f) Impact of Tg6F on changes over time in sCD14 (e) and sCD163 (f) in NSG BLT mouse model of chronic treated HIV. On day 56, postinfection (4–8 weeks on potent ART) and on day 112 postinfection (8–10 weeks of potent ART and Tg6F) blood was collected, plasma was prepared, and human biomarkers of monocyte activation (h-sCD14 and h-sCD163) were determined by Luminex immunoassays as in Methods. The change (Δ or delta) between day 56 and day 112 in h-sCD14 (Δh-sCD14) (e) and h-sCD163 (Δh-sCD163) (f) were determined for each mouse. The Mann–Whitney test was used to compare measures cross-sectionally at terminal endpoint and the change (Δ or delta) between day 56 and day 112 (Δh-sCD14 and Δh-sCD163) among two groups ($^*P < 0.05$, $^{**}P < 0.01$, $^{***}P < 0.001$). ART, antiretroviral therapy; GVHD, graft-versus-host.

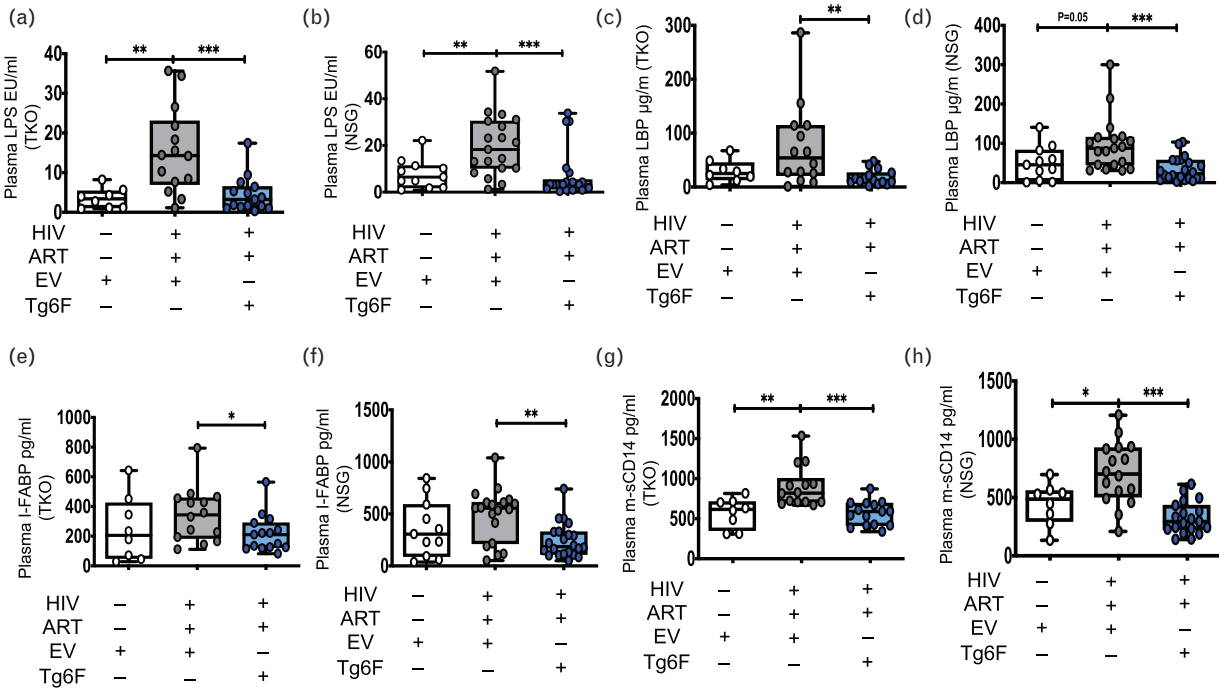

Fig. 2. Tg6F attenuates microbial translocation and gut barrier dysfunction in independent humanized mouse models of chronic treated HIV infection. TKO C57 ($n = 38$) and NSG ($n = 52$) humanized mice were constructed, infected with HIV and treated with ART, control transgenic tomato concentrate (EV) or Tg6F as described in Fig. 1. Whole blood from each mouse was collected, plasma was prepared, and murine plasma biomarkers of bacterial translocation and gut barrier dysfunction that are known predictors of morbidity in chronic treated HIV, were determined. Lipopolysaccharide (LPS) was quantified by endpoint chromogenic limulus amoebocyte lysate assay. Lipopolysaccharide-binding protein (LBP) and intestinal fatty acid-binding protein (I-FABP) were determined by ELISA. Murine plasma sCD14 levels were determined by Luminex. Data represent box and whiskers with minimum, median, and maximum values of murine plasma LPS (endotoxin units per milliliter; EU/ml) (a and b), LBP (µg/ml) (c and d), I-FABP (e and f), and plasma murine sCD14 (pg/ml) (g and h) in TKO (a, c, e, and g) and NSG (b, d, f, and h) humanized mice ($n = 8$–22 mice per group). The Mann–Whitney test was used to compare two groups ($^*P < 0.05$, $^{**}P < 0.01$, $^{***}P < 0.001$). TKO, triple knockout.

dysfunction (m-sCD14, LPS) but not LPS-binding protein (LBP) and m-IFABP, were increased in both NSG and TKO BLT HIV^+ART^+ mice compared with HIV^- mice (Fig. 2a–h).

Tg6F does not attenuate HIV-1 viral replication in bone marrow/liver/thymus model of HIV

We hypothesized that an oral intervention like apoA-I mimetic peptides that attenuate inflammatory phenotype of M/M [26] and directly bind microbial products like LPS and bioactive lipids [5,27,28] that interact with gut M/M and activate them, may attenuate inflammation and M/M activation in chronic treated HIV. To test our hypothesis, we cotreated HIV^+ART^+ NSG BLT mice fed chow diet with 0.06% Tg6F (wt/wt) with systemic ART for 10 weeks. To ensure that the effectiveness of Tg6F was because of the presence of 6F, which is not present in EV [6,8], the uninfected (HIV^-) and HIV^+ART^+ mice were all fed the chow diet that contained control transgenic tomato concentrate (EV) at the same dose as Tg6F (0.06% by weight). Given prior data that apoA-I and its amphipathic helix peptide analogues inhibit HIV-1-induced syncytium formation [29], we first tested whether Tg6F has direct antiviral effect *in vivo* in HIV-1-infected viremic humanized NSG mice.

Tg6F for 2 weeks did not impact plasma viremia in NSG BLT mice (Supplemental Figure 2a, http://links.lww.com/QAD/B945). Given that apoA-I mimetics may be a valuable therapeutic intervention to improve gut dysfunction and immune activation in the setting of potent ART and suppressed viremia, we also started Tg6F treatment in TKO BLT mice after the viremia was suppressed by ART, which was 4 weeks after the start of the experiment.

Tg6F attenuates monocytes/macrophages activation in bone marrow/liver/thymus models of HIV

Tg6F therapy for up to 14 weeks in NSG BLT mice attenuated sCD14 (Fig. 1c) and sCD163 (Fig. 1d) in HIV^+ART^+ $Tg6F^+$ compared with $HIV^+ART^+EV^+$ mice. Tg6F attenuated sCD14 (Supplemental Figure 3a, http://links.lww.com/QAD/B945) and sCD163 (Supplemental Figure 3b, http://links.lww.com/QAD/B945)

in HIV^+ART^+ $Tg6F^+$ NSG BLT compared with $HIV^+ART^+EV^+$ NSG BLT mice as early as 4 weeks after suppression of plasma viremia. Similar results were seen with TKO BLT mice (Supplemental Figure 3c and d, http://links.lww.com/QAD/B945). HIV^+ART^+ $Tg6F^+$ BLT mice had higher reduction in sCD14 (Δh-sCD14) and sCD163 (Δh-sCD163) over time compared with $HIV^+ART^+EV^+$ BLT mice in both NSG (Fig. 1e and f) and TKO mice (Supplemental Figure 4a and b, http://links.lww.com/QAD/B945).

Tg6F attenuates gut barrier dysfunction in bone marrow/liver/thymus models of HIV

We next hypothesized that Tg6F attenuates immune activation in treated HIV through reducing gut barrier dysfunction. Compared with $HIV^+ART^+EV^+$ mice, the $HIV^+ART^+Tg6F^+$ mice expressed lower levels of plasma m-sCD14, LPS, LBP, and m-IFABP in both NSG and TKO BLT mice (Fig. 2a–h). Confirming our prior reports that Tg6F attenuates gut inflammation [6,8,9,30], Tg6F attenuated gut barrier dysfunction in BLT models of chronic treated HIV.

Tg6F attenuates oxidized lipoproteins as instigators of immune activation in bone marrow/liver/thymus models of HIV

Given that IFABP is a cellular lipid chaperone that binds lipids [31] and prior data that oxidized lipoproteins are associated with immune activation in chronic treated HIV [32,33], we hypothesized that alterations in plasma and gut oxidized lipoproteins contribute to immune activation in chronic treated HIV. We assessed plasma and gut levels of murine oxidized high-density and low-density lipoproteins (HDLox and LDLox) by ELISA or a fluorometric method (plasma HDLox) (Fig. 3a–g). There were no differences in plasma levels of lipids including HDL-C and LDL-C among all groups in both BLT models (Supplemental Figure 5a–h, http://links.lww.com/QAD/B945). Plasma and gut HDLox and LDLox were increased in HIV^+ART^+ mice compared with HIV^- mice in both NSG and TKO BLT mice (Fig. 3a–g). Intestinal LDLox was associated with plasma m-sCD14, h-sCD14 but not with h-sCD163 (Supplemental Figure 6c, g and k, http://links.lww.com/QAD/B945). Gut HDLox was associated with h-sCD163 but not with m-sCD14 and

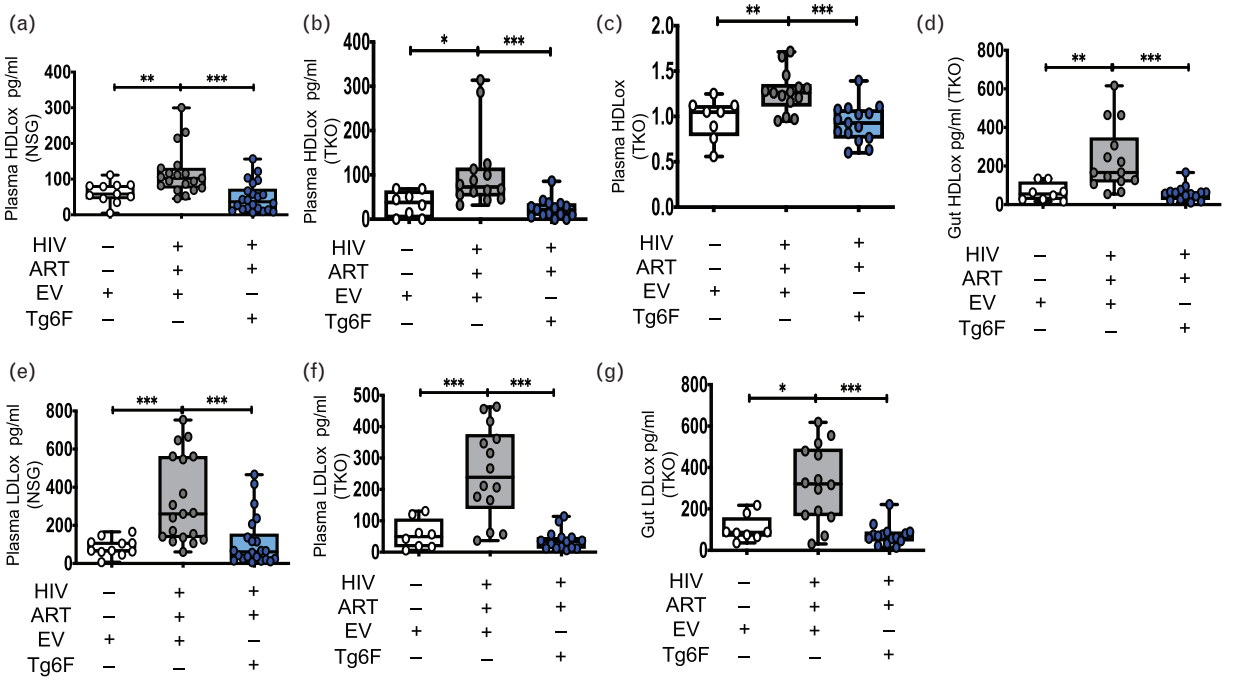

Fig. 3. Tg6F attenuates increases in plasma and gut oxidized lipoproteins driven by HIV and/or antiretroviral therapy in chronic treated HIV infection. TKO C57 ($n = 38$) and NSG ($n = 52$) humanized mice were constructed, infected with HIV and treated with ART, control transgenic tomato concentrate (EV) or Tg6F as described in Fig. 1. Whole blood and small intestine from each mouse were collected, plasma and tissue homogenates were prepared and murine plasma and gut oxidized lipoproteins [oxidized high-density lipoprotein (HDLox), oxidized low-density lipoprotein (LDLox)] were determined in plasma of TKO and NSG BLT mice and homogenate of small intestine from TKO BLT mice as in methods by ELISA (a, b, d, and e–h). HDLox (normalized ratio to control, no units) was determined in plasma of TKO BLT mice with a fluorometric method (c) as described in the supplemental material. Data represent box and whiskers with minimum, median and maximum values ($n = 8$–22 mice per group) of plasma HDLox (a–c), gut HDLox (d), plasma LDLox (e and f) and gut LDLox (g) in NSG (a and e) and TKO (b, c, d, f–h). The Mann–Whitney test was used to compare two groups ($^*P < 0.05$, $^{**}P < 0.01$, $^{***}P < 0.001$).

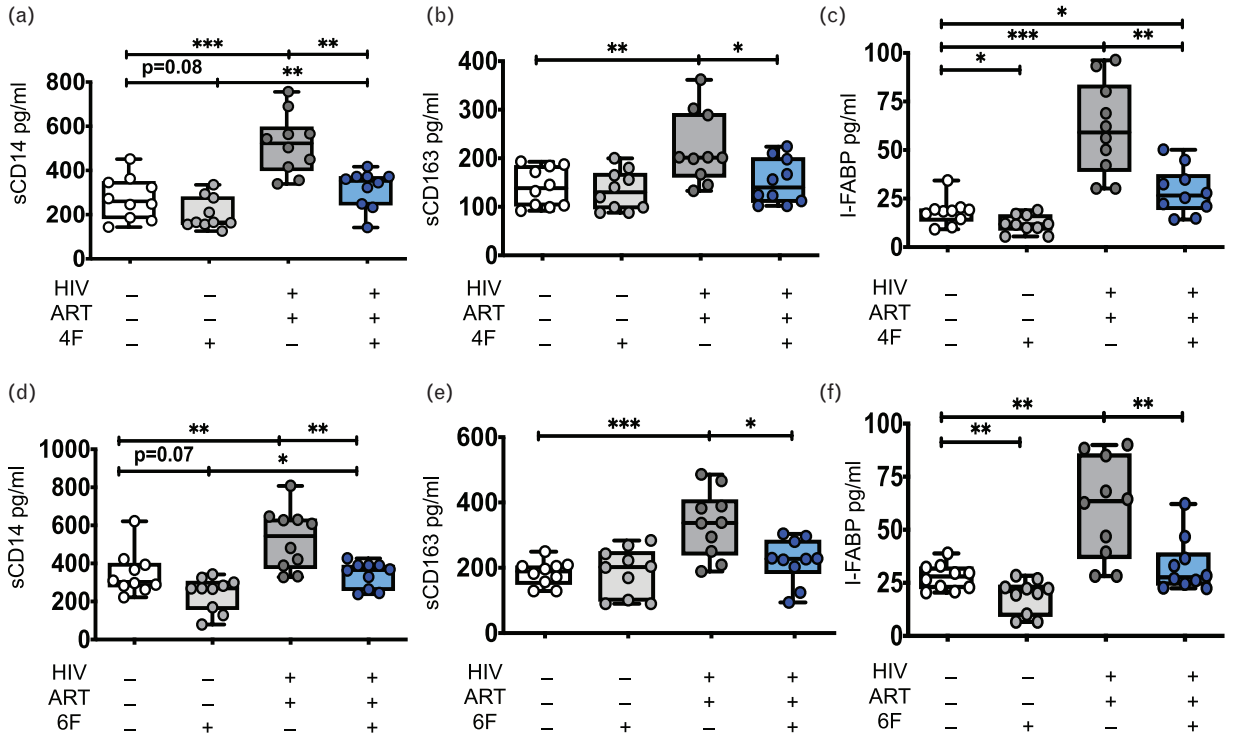

Fig. 4. Apolipoprotein A-I mimetic peptides attenuates ex-vivo biomarkers of immune activation and gut injury derived from gut explants of uninfected and HIV-infected antiretroviral-treated participants. Gut biopsies were obtained from uninfected ($n = 10$) and HIV-infected participants on potent ART ($n = 10$) and gut explants were treated with 4F or 6F apoA-I mimetic peptides or sham peptide at concentration 100 μg/ml for 72 h as in methods. Supernatants were collected and protein levels of secreted sCD14, sCD163 were determined in supernatants by Luminex immunoassays. I-FABP was determined by ELISA. The first group included gut explants from uninfected participants treated with sham peptide, white boxes, and datapoints, HIV^- ($n = 10$). The second group included gut explants from uninfected participants treated with 4F (a–c) or 6F (d–f), light grey boxes and datapoints, HIV^- ($n = 10$). The third group included gut explants from HIV-infected participants who received ART; these explants were treated with sham peptide, dark grey boxes and datapoints, HIV^+ART^+ ($n = 10$). The fourth group included gut explants from HIV-infected participants who received ART; these explants were treated with 4F (a–c) or 6F (d–f), blue boxes and datapoints, $HIV^+ART^+4F^+$ or $HIV^+ART^+6F^+$ ($n = 10$). Gut biopsies from the same participants were used for experiments with 4F and 6F. Data represent box and whiskers with minimum, median, and maximum values of sCD14 (a and d), sCD163 (b and e) and I-FABP (c and f) ($n = 10$ per group). Datapoints represent mean of three gut biopsies per participant. The Mann–Whitney test was used to compare two groups ($^*P < 0.05$, $^{**}P < 0.01$, $^{***}P < 0.001$). apoA-I, apolipoprotein A-I; ART, antiretroviral therapy.

h-sCD14 (Supplemental Figure 6a, e, and i, http://links.lww.com/QAD/B945). These associations were lost in the $HIV^+ART^+Tg6F^+$ groups (Supplemental Figure 6d, h, j, and l, http://links.lww.com/QAD/B945) given that Tg6F treatment rescued all increases in plasma and gut HDLox and LDLox in chronic treated HIV (Fig. 3a–g).

4F attenuates ex-vivo biomarkers of immune activation and gut injury derived from gut explants of uninfected and HIV-infected antiretroviral therapy-treated participants

Tg6F is not yet available for clinical trial in humans. Given that 4F has been shown to be well tolerated in humans when given orally [10], we tested whether 4F attenuates ex-vivo biomarkers of immune activation and gut injury derived from colon tissues of uninfected ($n = 10$) and HIV infected ($n = 10$) ART-treated 50–60 years old white men without clinical morbidity, on potent ART. Supernatants from gut explants of HIV^+ participants had higher protein levels of sCD14, sCD163, and IFABP compared with gut explants of uninfected participants (Fig. 4a–f). Unlike treatment with the sham peptide, treatment of gut explants with 4F for 72 h, attenuated levels of sCD14, sCD163, and I-FABP from gut explants of HIV^+ participants. 4F also attenuated levels of I-FABP (Fig. 4c) and tended ($P = 0.08$) to reduce levels of sCD14 (Fig. 4a) from gut explants of uninfected participants. Similar data like 4F were observed with 6F (Figure 4d–f). Overall, our complementary BLT mouse and ex-vivo human studies, demonstrated that apoA-I mimetic peptides attenuate oxidized lipoproteins, intestinal barrier dysfunction, and macrophage activation in chronic treated HIV (Fig. 5).

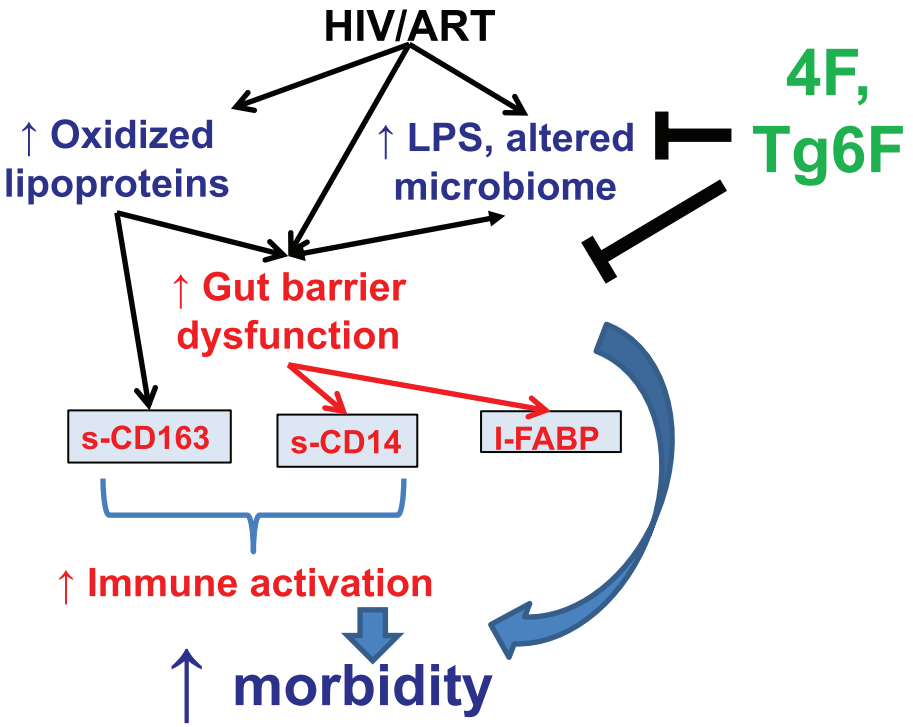

Fig. 5. Overall hypothesis. HIV, ART, oxidized lipoproteins (HDLox, LDLox), and microbial products (such as LPS) collectively drive gut barrier dysfunction (increased circulating I-FABP) and macrophage activation (increased circulating sCD14, sCD163) in chronic treated HIV. ApoA-I mimetic peptides, such as 4F and Tg6F bind LPS and attenuate formation of oxidized lipoproteins in the gut, reducing macrophage activation, gut barrier dysfunction, and ultimately morbidity in chronic treated HIV. ART, antiretroviral therapy; HDLox, oxidized high-density lipoprotein; LDLox, oxidized low-density lipoprotein; LPS, lipopolysaccharide.

Discussion

Herein, using mouse models of chronic treated HIV [15,16,34] and human gut explants, we demonstrate that apoA-I mimetics reduced oxidized lipoproteins (HDLox, LDLox) and biomarkers of intestinal barrier dysfunction (LPS, LBP, I-FABP) and immune activation (sCD163, sCD14) in chronic treated HIV. Despite the limitations of humanized mouse models, we demonstrated the capacity of independent BLT mouse models to support HIV infection, express biomarkers of intestinal barrier dysfunction and M/M activation in the setting chronic treated HIV and consistently respond to clinically relevant ART. The component of Tg6F accounting for the beneficial effects on M/M activation is the 6F peptide, as EV [6,8] had no effect on biomarkers of M/M activation in chronic treated HIV. Tg6F seem to work exclusively in the gut [6–9]. The safety and pharmacokinetics of oral apoA-I mimetic peptides have been tested in humans [10] and mice [6–9]. ApoA-I mimetic peptides seem to achieve higher concentration in the proximal small intestine [6–9]. Our data (Fig. 5) support the concept that therapeutic targeting of intestinal barrier dysfunction, LPS, and oxidized lipoproteins, may have a favorable impact on immune activation that can complement ART to attenuate development of comorbidities like CVD in chronic treated HIV.

Our robust experimental approach provides important preclinical insight into the therapeutic impact of apoA-I mimetics on immune activation in chronic HIV. Given that GVHD is associated with increased levels of sCD163 [35], we excluded NSG mice with clinical GVHD and we also included studies with TKO BLT mice [18–20]. To ensure that cohort differences do not confound interpretation of data, we assessed the impact of Tg6F both cross-sectionally across different cohorts and longitudinally within the same cohort, in independent BLT models. Although low level of HIV-1 replication may be seen in the BLT models, we demonstrated that Tg6F did not have an impact on viral replication and the impact on biomarkers of immune activation was because of effect of Tg6F on oxidized lipoproteins. The favorable impact of apoA-I mimetics on M/M activation was also shown in gut explants from HIV-infected participants on potent ART. Gut explants are physiologically meaningful and do not have the limitations of several other ex-vivo gut models [36]. In all models, we consistently found that apoA-I mimetics attenuated release of sCD14 and sCD163, suggesting a favorable effect on immune activation in chronic treated HIV.

Our data that apoA-I mimetics attenuated oxidized lipoproteins in parallel to M/M activation, are consistent with prior human studies by us and others that oxidized

lipoproteins, that carry oxidized lipids, are associated with immune dysfunction in chronic treated HIV [32,33]. Although HDL is generally an anti-inflammatory lipoprotein during systemic inflammation, it can be oxidized (HDLox) and becomes dysfunctional [12,25,37,38]. Oxidized LDL also carries oxidized lipids and like HDLox may also contribute to immune activation in HIV [32,33]. Consistent with this evidence, we showed that the associations between plasma and gut bioactive lipids with biomarkers of gut impairment, immune activation, and inflammation in the $HIV^+ART^+EV^+$ group were attenuated in the $HIV^+ART^+Tg6F^+$ group with an intervention that directly attenuates oxidized lipoproteins. These results suggest a causal relationship between increases in immune activation and oxidized lipoproteins in chronic treated HIV.

We have previously shown that Tg6F attenuates the accumulation of oxidized phospholipids in the small intestine and inflammation in murine models of disease [30]. Tg6F decreased small intestine enterocyte and plasma levels of LBP, CD14, TLR4, and MyD88 [39]. Activation of the TLR pathway by LPS is dependent on the co-localization of TLR4 and CD14 in lipid rafts that permit the activation of downstream signaling that culminate in NF-κB activation and the synthesis of pro-inflammatory cytokines [40]. Bioactive lipids may also disrupt epithelial cell tight junctions either directly [41] or through lipid raft disruption [42,43] or TNF-α signaling [44]. ApoA-I mimetics like 4F also regulate in-vitro expression of FABPs (fatty-acid-binding proteins), which act as lipid chaperones in the cell [45]. Thus, Tg6F through favorable effects on oxidized lipoproteins and LPS may alter epithelial and immune cells in the lamina propria of the gut. These favorable effects of Tg6F contribute to attenuation of M/M activation in chronic treated HIV. Notably, in a prior clinical trial of 4F in humans, 4F was given parenterally and not orally [11] and did not improve HDL functionality [11]. Further work from our group demonstrated that apoA-I mimetics like 4F and 6F work primarily in the gut to inhibit gut inflammation and M/M activation [6–9], and oral apoA-I mimetics demonstrate therapeutic efficacy in several inflammatory diseases including cancer, cardiovascular, and inflammatory bowel disease [6–9]. Providing the same dose (mg/kg) of Tg6F to humans as was used in these studies with mice would require only two tablespoons three times daily making this a practical approach for testing Tg6F in the treatment of inflammation in chronic treated HIV [7].

Our study has several limitations. First, not all aspects of human HIV infection can be modeled accurately in humanized mice. Most macrophages are of murine origin and resistant to HIV infection. Unlike humans, most human M/M in the BLT models are not in the gastrointestinal tract (overall there is low engraftment) [15,16,34]. Humanized mice are less commonly used to study immune activation because of important immunologic differences including GVHD and the lack of well-formed secondary lymphoid tissues of human cell origin. However, we included GVHD-resistant mice and focused on M/M rather than lymphocyte activation. Second, there are major differences in the microbiome between mouse and human [46] and the humanized mice may not recapitulate the same disorder of microbial translocation as in HIV-infected individuals; we did not perform detailed microbiome studies. Third, the gut barrier dysfunction in humanized mice reflects effects from irradiation, GVHD, HIV, and ART. Thus, semiquantitative histologic assessments of gut barrier integrity were not performed and focused only on clinically relevant measures of bacterial translocation. As with all in-vitro model systems, gut explants cannot fully recapitulate the in-vivo conditions and only examine early effects of signaling. However, ex-vivo addition of 4F in gut explants is the only preclinical approach in humans at this time. Finally, given the above limitations, we did not assess changes in the functional phenotype of myeloid cells in circulation or in gut tissue following administration of apoA-I mimetics. Thus, it is possible that our findings could also be explained by other underlying mechanistic pathways that were not studied in our preclinical models. A clinical trial is needed to assess the impact of oral 4F on the microbiome, gut barrier integrity, and key signaling pathways that drive immune activation in chronic treated HIV.

Despite these limitations, our consistent preclinical data support the hypothesis that apoA-I mimetic peptides can attenuate a cycle of production of bioactive lipids and microbial products that contribute to immune activation and morbidity in chronic treated HIV. 4F has been shown to be well tolerated in humans when given orally [10] or parenterally [11] and can be translated to HIV infected persons for a future clinical trial in chronic treated HIV. We offer evidence of the possible translational value of apoA-I mimetic peptides as therapy for morbidity in chronic treated HIV, while adding to our understanding of their protective mechanisms.

Acknowledgements

Antiviral compounds were generously supplied by Gilead Sciences. The flow cytometry machine used in the study was purchased through the UCLA Center for AIDS Research (P30AI28697) grant.

Funding statement: this work was supported in part by NIH grants R01AG059501, R21AI36708, R21HL134444, R03AG059462, R03AG059462, K08AI108272 (to T.K.), R01HL071776 (to S.T.R.), R01HL148286 (to A.M.F.); the Castera, Laubisch, and Milt Grey funds at UCLA. Research reported in this publication was also supported

by NIH grants AI078806 and AI110306-01 (to S.K.); NIH/NIAID 1U19AI117941-01; AmfAR 108929-56-RGRL, 108688-54-RGRL, 109577-62-RGRL (Kitchen-PI), the UCLA Center for AIDS Research (P30AI28697); the California Institute for Regenerative Medicine (TR4-06845) and California HIV/AIDS Research Program (OS17-LA-002 to T.K.) and Campbell Foundation (T.K.). The following reagent was obtained through the NIH AIDS Reagent Program, Division of AIDS, NIAID, NIH: HIV-1 89.6 Virus from Dr Ronald Collman.

Author contributions: T.K. conceived the project, which had leadership from STR. T.K. designed, analyzed experiments and wrote the manuscript with contributions from W.M and STR. R.E, M.S., H.R., R.V., H.P., K.A., S.S.R. helped conduct the animal studies and maintain the animal colonies. R.H., P.H., J.P., and D.M. did lipid extractions. R.H., M.S., J.P., and P.H. did immunoassays and lipid experiments. R.E., H.R., M.S., W.M., H.P. did flow cytometry experiments. R.H., M.S., and K.A. did PCR experiments. D.M. helped develop the LC-MS/MS lipid analysis methods. G.V. and C.A. helped prepare Tg6F diets. S.G.K. provided guidance, feedback, and financial support (UCLA Humanized Mouse Core). A.M.F. provided guidance, feedback, supervision, edited the manuscript, and financial support. S.T.R. provided guidance and feedback regarding the overall study and individual experiments, edited the manuscript, and provided laboratory and financial support.

Conflicts of interest

A.M.F. and S.T.R. are principals in Bruin Pharma, and A.M.F. is an officer in Bruin Pharma. All other authors have declared that no conflict of interest exists.

References

1. Lederman MM, Funderburg NT, Sekaly RP, Klatt NR, Hunt PW. **Residual immune dysregulation syndrome in treated HIV infection.** *Adv Immunol* 2013; **119**:51–83.
2. Sandler NG, Wand H, Roque A, Law M, Nason MC, Nixon DE, *et al*., INSIGHT SMART Study Group. **Plasma levels of soluble CD14 independently predict mortality in HIV infection.** *J Infect Dis* 2011; **203**:780–790.
3. Knudsen TB, Ertner G, Petersen J, Moller HJ, Moestrup SK, Eugen-Olsen J, *et al*. **Plasma soluble CD163 level independently predicts all-cause mortality in HIV-1-infected individuals.** *J Infect Dis* 2016; **214**:1198–1204.
4. Gilbert JM, Fitch KV, Grinspoon SK. **HIV-related cardiovascular disease, statins, and the REPRIEVE Trial.** *Top Antivir Med* 2015; **23**:146–149.
5. Navab M, Shechter I, Anantharamaiah GM, Reddy ST, Van Lenten BJ, Fogelman AM. **Structure and function of HDL mimetics.** *Arterioscler Thromb Vasc Biol* 2010; **30**:164–168.
6. Chattopadhyay A, Navab M, Hough G, Gao F, Meriwether D, Grijalva V, *et al*. **A novel approach to oral apoA-I mimetic therapy.** *J Lipid Res* 2013; **54**:995–1010.
7. Chattopadhyay A, Grijalva V, Hough G, Su F, Mukherjee P, Farias-Eisner R, *et al*. **Efficacy of tomato concentrates in mouse models of dyslipidemia and cancer.** *Pharmacol Res Perspect* 2015; **3**:e00154.
8. Chattopadhyay A, Yang X, Mukherjee P, Sulaiman D, Fogelman HR, Grijalva V, *et al*. **Treating the intestine with oral ApoA-I mimetic Tg6F reduces tumor burden in mouse models of metastatic lung cancer.** *Sci Rep* 2018; **8**:9032.
9. Meriwether D, Sulaiman D, Volpe C, Dorfman A, Grijalva V, Dorreh N, *et al*. **Apolipoprotein A-I mimetics mitigate intestinal inflammation in COX2-dependent inflammatory bowel disease model.** *J Clin Invest* 2019; **130**:3670–3685.
10. Bloedon LT, Dunbar R, Duffy D, Pinell-Salles P, Norris R, DeGroot BJ, *et al*. **Safety, pharmacokinetics, and pharmacodynamics of oral apoA-I mimetic peptide D-4F in high-risk cardiovascular patients.** *J Lipid Res* 2008; **49**:1344–1352.
11. Watson CE, Weissbach N, Kjems L, Ayalasomayajula S, Zhang Y, Chang I, *et al*. **Treatment of patients with cardiovascular disease with L-4F, an Apo-A1 mimetic, did not improve select biomarkers of HDL function.** *J Lipid Res* 2011; **52**:361–373.
12. Kelesidis T, Yang OO, Currier JS, Navab K, Fogelman AM, Navab M. **HIV-1 infected patients with suppressed plasma viremia on treatment have pro-inflammatory HDL.** *Lipids Health Dis* 2011; **10**:35.
13. Evans DT, Silvestri G. **Nonhuman primate models in AIDS research.** *Curr Opin HIV AIDS* 2013; **8**:255–261.
14. Potash MJ, Chao W, Bentsman G, Paris N, Saini M, Nitkiewicz J, *et al*. **A mouse model for study of systemic HIV-1 infection, antiviral immune responses, and neuroinvasiveness.** *Proc Natl Acad Sci U S A* 2005; **102**:3760–3765.
15. Melkus MW, Estes JD, Padgett-Thomas A, Gatlin J, Denton PW, Othieno FA, *et al*. **Humanized mice mount specific adaptive and innate immune responses to EBV and TSST-1.** *Nat Med* 2006; **12**:1316–1322.
16. Zhen A, Rezek V, Youn C, Lam B, Chang N, Rick J, *et al*. **Targeting type I interferon-mediated activation restores immune function in chronic HIV infection.** *J Clin Invest* 2017; **127**:260–268.
17. Hofer U, Schlaepfer E, Baenziger S, Nischang M, Regenass S, Schwendener R, *et al*. **Inadequate clearance of translocated bacterial products in HIV-infected humanized mice.** *PLoS Pathog* 2010; **6**:e1000867.
18. Lavender KJ, Messer RJ, Race B, Hasenkrug KJ. **Production of bone marrow, liver, thymus (BLT) humanized mice on the C57BL/6 Rag2(−/−)gammac(−/−)CD47(−/−) background.** *J Immunol Methods* 2014; **407**:127–134.
19. Lavender KJ, Pace C, Sutter K, Messer RJ, Pouncey DL, Cummins NW, *et al*. **An advanced BLT-humanized mouse model for extended HIV-1 cure studies.** *AIDS* 2018; **32**:1–10.
20. Lavender KJ, Pang WW, Messer RJ, Duley AK, Race B, Phillips K, *et al*. **BLT-humanized C57BL/6Rag2-/-gammac-/-CD47-/- mice are resistant to GVHD and develop B- and T-cell immunity to HIV infection.** *Blood* 2013; **122**:4013–4020.
21. Marsden MD, Kovochich M, Suree N, Shimizu S, Mehta R, Cortado R, *et al*. **HIV latency in the humanized BLT mouse.** *J Virol* 2012; **86**:339–347.
22. Satheesan S, Li H, Burnett JC, Takahashi M, Li S, Wu SX, *et al*. **HIV replication and latency in a humanized NSG mouse model during suppressive oral combinational antiretroviral therapy.** *J Virol* 2018; **92**:e02118–17.
23. Scotland RS, Stables MJ, Madalli S, Watson P, Gilroy DW. **Sex differences in resident immune cell phenotype underlie more efficient acute inflammatory responses in female mice.** *Blood* 2011; **118**:5918–5927.
24. Fletcher PS, Elliott J, Grivel JC, Margolis L, Anton P, McGowan I, Shattock RJ. **Ex vivo culture of human colorectal tissue for the evaluation of candidate microbicides.** *AIDS* 2006; **20**:1237–1245.
25. Kelesidis T, Roberts CK, Huynh D, Martinez-Maza O, Currier JS, Reddy ST, Yang OO. **A high throughput biochemical fluorometric method for measuring lipid peroxidation in HDL.** *PLoS One* 2014; **9**:e111716.
26. Smythies LE, White CR, Maheshwari A, Palgunachari MN, Anantharamaiah GM, Chaddha M, *et al*. **Apolipoprotein A-I mimetic 4F alters the function of human monocyte-derived macrophages.** *Am J Physiol Cell Physiol* 2010; **298**:C1538–C1548.
27. Van Lenten BJ, Wagner AC, Jung CL, Ruchala P, Waring AJ, Lehrer RI, *et al*. **Anti-inflammatory apoA-I-mimetic peptides bind oxidized lipids with much higher affinity than human apoA-I.** *J Lipid Res* 2008; **49**:2302–2311.

28. Navab M, Anantharamaiah GM, Reddy ST, Fogelman AM. **Apolipoprotein A-I mimetic peptides and their role in atherosclerosis prevention.** *NatClinPractCardiovascMed* 2006; **3**:540–547.
29. Owens BJ, Anantharamaiah GM, Kahlon JB, Srinivas RV, Compans RW, Segrest JP. **Apolipoprotein A-I and its amphipathic helix peptide analogues inhibit human immunodeficiency virus-induced syncytium formation.** *J Clin Invest* 1990; **86**:1142–1150.
30. Chattopadhyay A, Navab M, Hough G, Grijalva V, Mukherjee P, Fogelman HR, *et al*. **Tg6F ameliorates the increase in oxidized phospholipids in the jejunum of mice fed unsaturated LysoPC or WD.** *J Lipid Res* 2016; **57**:832–847.
31. Furuhashi M, Ishimura S, Ota H, Miura T. **Lipid chaperones and metabolic inflammation.** *Int J Inflam* 2011; **2011**:642612.
32. Kelesidis T, Jackson N, McComsey GA, Wang X, Elashoff D, Dube MP, *et al*. **Oxidized lipoproteins are associated with markers of inflammation and immune activation in HIV-1 infection.** *AIDS* 2016; **30**:2625–2633.
33. Zidar DA, Juchnowski S, Ferrari B, Clagett B, Pilch-Cooper HA, Rose S, *et al*. **Oxidized LDL levels are increased in HIV infection and may drive monocyte activation.** *J Acquir Immune Defic Syndr* 2015; **69**:154–160.
34. Wahl A, Victor Garcia J. **The use of BLT humanized mice to investigate the immune reconstitution of the gastrointestinal tract.** *J Immunol Methods* 2014; **410**:28–33.
35. Inamoto Y, Martin PJ, Paczesny S, Tabellini L, Momin AA, Mumaw CL, *et al*. **Association of plasma CD163 concentration with de novo-onset chronic graft-versus-host disease.** *Biol Blood Marrow Transplant* 2017; **23**:1250–1256.
36. Pearce SC, Coia HG, Karl JP, Pantoja-Feliciano IG, Zachos NC, Racicot K. **Intestinal in vitro and ex vivo models to study host-microbiome interactions and acute stressors.** *Front Physiol* 2018; **9**:1584.
37. Navab M, Reddy ST, Van Lenten BJ, Fogelman AM. **HDL and cardiovascular disease: atherogenic and atheroprotective mechanisms.** *Nat Rev Cardiol* 2011; **8**:222–232.
38. Kelesidis T, Currier JS, Huynh D, Meriwether D, Charles-Schoeman C, Reddy ST, *et al*. **A biochemical fluorometric method for assessing the oxidative properties of HDL.** *J Lipid Res* 2011; **52**:2341–2351.
39. Mukherjee P, Hough G, Chattopadhyay A, Grijalva V, O'Connor EI, Meriwether D, *et al*. **Role of enterocyte stearoyl-Co-A desaturase-1 in LDLR-null mice.** *J Lipid Res* 2018; **59**:1818–1840.
40. Triantafilou M, Gamper FG, Haston RM, Mouratis MA, Morath S, Hartung T, *et al*. **Membrane sorting of toll-like receptor (TLR)-2/6 and TLR2/1 heterodimers at the cell surface determines heterotypic associations with CD36 and intracellular targeting.** *J Biol Chem* 2006; **281**:31002–31011.
41. Chen-Quay SC, Eiting KT, Li AW, Lamharzi N, Quay SC. **Identification of tight junction modulating lipids.** *J Pharm Sci* 2009; **98**:606–619.
42. Chen ML, Ge Z, Fox JG, Schauer DB. **Disruption of tight junctions and induction of proinflammatory cytokine responses in colonic epithelial cells by Campylobacter jejuni.** *Infect Immun* 2006; **74**:6581–6589.
43. Levitan I, Shentu TP. **Impact of oxLDL on cholesterol-rich membrane rafts.** *J Lipids* 2011; **2011**:730209.
44. Freour T, Jarry A, Bach-Ngohou K, Dejoie T, Bou-Hanna C, Denis MG, *et al*. **TACE inhibition amplifies TNF-alpha-mediated colonic epithelial barrier disruption.** *Int J Mol Med* 2009; **23**:41–48.
45. Smathers RL, Petersen DR. **The human fatty acid-binding protein family: evolutionary divergences and functions.** *Hum Genomics* 2011; **5**:170–191.
46. Hugenholtz F, de Vos WM. **Mouse models for human intestinal microbiota research: a critical evaluation.** *Cell Mol Life Sci* 2018; **75**:149–160.